This article has been accepted for publication in a future issue of this journal, but has not been fully edited. Content may change prior to final publication. Citation information: DOI 10.1109/TIP.2017.2716840, IEEE Transactions on Image Processing

A Novel Fast Tensor-Based Preconditioner for Image Restoration

Mansoor Rezghi

***Abstract*—Image restoration is one of the main parts of image processing. Mathematically, this problem can be modeled as a large scale structured ill-posed linear system. Ill-posedness of this problem results in low convergence rate of iterative solvers. For speeding up the convergence, preconditioning usually is used. Despite the existing preconditioners for image restoration which are constructed based on approximations of the blurring matrix, in this paper, we propose a novel preconditioner with a different viewpoint. Here, we show that image restoration problem can be modeled as a tensor contractive linear equation. This modeling enables us to propose a new preconditioner based on an approximation of the blurring tensor operator. Due to the particular structure of the blurring tensor for zero boundaries, we show that the truncated higher order singular value decomposition(HOSVD) of the blurring tensor is obtained very fast and so could be used as a preconditioner. Experimental results confirm the efficiency of this new preconditioner in image restoration and its outperformance in comparison with the other well-known preconditioners.**

***Index Terms*—Image restoration, Iterative methods, Preconditioning, Tensor, HOSVD, Lanczos bidiagonalization**

I. Introduction

Image restoration is one of the main parts of image processing [1], [2]. It is the process of recovering a faithful representation of an original scene from blurred and noisy image data. Mathematically, space invariant blurring process can modeled as

$$y(s) = \int_{-\infty}^{\infty} p(s-t)x(t)dt + e, \tag{I.1}$$

where x, y and e are the exact, noisy blurred images and the noise term, respectively. Also $p(.)$ is a function that specifies how the points in the image are blurred called point spread function (PSF)[1]. This problem is ill-posed and so very sensitive to the noise on the right-hand side. The discrete version of the blurring procedure can be modeled as the following large scale ill-posed linear system,

$$\mathbf{y} = A\mathbf{x}, \quad \mathbf{y} = \mathbf{b} + \mathbf{e}, \tag{I.2}$$

where A is a blurred matrix and its structure depends on the PSF array and boundary conditions. In this paper, we consider zero boundary condition and so the blurring matrix A becomes a multilevel block Toeplitz matrix [1].

Usually, iterative methods are used to solve this structured large scale and ill-posed linear system [1], [2], [3], [4], [5]. Therefore, at each step of iterative methods, the matrix-vector multiplication can be carried out very fast by FFT, without using the explicit form of the blurring matrix, which reduces the computational and storage costs [4]. Also, iterative methods like CGLS (Conjugate gradient for least square problems) have regularization property which is known as semi-convergency [6], [7].

Despite these excellent properties, usually their convergence rate is low and preconditioning should be applied to improve the convergence rate [1]. The preconditioning is the process of substituting the linear system (I.2) with

$$M^{-1}A\mathbf{x} = M^{-1}\mathbf{y},$$

which the rate of convergence of iterative methods for this system is better than the original system (I.2). Here, the matrix M is the preconditioner matrix and usually considered as an approximation of A [8], [9], [10]. The concept of preconditioning for discrete ill-posed problems differs from the standard preconditioning. The standard preconditioning tries to speed up the convergence by clustering the entire singular values of the preconditioned system around 1, while in the context of the ill-posed problems, the preconditioner should provide regularization property and only the large singular values need special attention. Therefore, in ill-posed problems, a preconditioner should able to improve the distribution and location of the large singular values and leave the rest of them to prevent the propagation of the noise in solution [3]. So, the truncated version of singular or eigenvalue decomposition of the blurring matrix is an ideal preconditioner. But, its computation is very time-consuming and so is not reasonable. In the literature, different kinds of approximations have been proposed that implicitly approximate the blurring matrix in the space corresponding to large singular values (which called signal space). These preconditioning methods are dependent on the boundary conditions [11], [12]. Some preconditioners based on circulant approximation of the blurring matrix for zero boundary conditions(BCs) have been proposed in [13], [5]. In [3], the authors used incomplete Lanczos bidiagonalization process to find an approximation which could be utilized for all BCs. This is improved in [14]. Using the optimal keronecker product approximation of the blurring matrix is another approach which different preconditioners for various BCs have been proposed based on this approach in the recent years [15], [16], [17], [18]. The extensions of Kronecker based preconditioner for 3D image restoration has been done in [1], [19]. The quality of the preconditioners in this approach are usually better than circulant based preconditioners [15].

All of the mentioned methods are based on the approximation of the blurring matrix. In this paper, we propose a

M. Rezghi, Department of Computer Science, Tarbiat Modares University, Tehran-Iran e-mail: Rezghi@modares.ac.ir.

This article has been accepted for publication in a future issue of this journal, but has not been fully edited. Content may change prior to final publication. Citation information: DOI 10.1109/TIP.2017.2716840, IEEE Transactions on Image Processing

novel preconditioner with a different viewpoint based on tensor modelling. In recent years different tensor based methods has been used in image processing [20], [21], [22]. Here, we demonstrate that image restoration problem can be modeled as a contractive tensor- tensor equation, which its matricization is equal to matrix modeling in (I.2). This modeling enables us to construct new preconditioners based on approximations of the blurring tensor which could not be obtained with the matrix framework. We show that due to the structure of the blurring tensor, the HOSVD of the blurring tensor can be obtained very fast and approximation of its truncated version can be used as a preconditioner, which its computational complexity is comparable to other preconditioners like Kronecker product approximation based preconditioner.

We use this fast tensor-based preconditioner on some 2D and 3D image restoration problems. Experimental results confirm the high quality of this preconditioner. The novelty of this paper can be categorized in two cases: First, we give a new insight to image restoration problem based on tensor modeling. This viewpoint enables us to use different tensor approximations as a preconditioner. Secondly, we show that the HOSVD of the blurring tensor with zero boundary condition can be calculated very fast. So, using the truncated version of HOSVD of the blurring operator as preconditioner is reasonable.

The remainder of this paper is organized as the follows: Section II contains some basic concepts. In section III we propose our novel preconditioner based on tensor modeling. Section IV presents some experimental results.

II. Notations and preliminaries

Tensors can be considered as a generalization of vectors and matrices of high dimensions. We use calligraphic letters to denote the tensors, e.g, $\mathcal{A}, \mathcal{B}$. Let $\mathcal{A} \in \mathbb{R}^{I_1 \times I_2 \times I_3}$ denotes an order-3 tensor. Different "dimensions" of tensors are referred to as *modes*. We will use both standard subscripts and "MATLAB-like" notation to show tensor elements as follows:

$$\mathcal{A}(i,j,k) = a_{ijk}.$$

A fiber is a subtensor, where all indices but one are fixed. For example mode-2 fibers of $\mathcal{A}$, have following form

$$\mathcal{A}(i,:,j) \in \mathbb{R}^{I_2}.$$

The mode-n product of an order-M tensor $\mathcal{A} \in \mathbb{R}^{I_1 \times \ldots \times I_M}$ by a matrix $X \in \mathbb{R}^{K \times I_n}$ is defined as

$$\mathbb{R}^{I_1 \times \ldots I_{n-1} \times K \times I_{n+1} \times \ldots I_M} \ni \mathcal{B} = (X)_n \cdot \mathcal{A}, \qquad \text{(II.1)}$$

where,

$$b_{i_1,\ldots,i_n} = \sum_{l=1}^{I_n} x_{i_n,l} a_{i_1,\ldots,i_{n-1},l,i_{n+1},\ldots,i_M}.$$

This means that all mode-n fibers of $\mathcal{A}$ are multiplied by the matrix X. The notation (II.1) was suggested by Lim [23]. An alternative notation was earlier given in [24]. $(X)_n \cdot \mathcal{A}$ is the same as $\mathcal{A} \times_n X$ in that system. The Frobenius norm of the order-M tensor $\mathcal{A}$ can be defined as $\|\mathcal{A}\| = \left(\sum_{i_1,\ldots,i_M} a^2_{i_1 \ldots i_M}\right)^{1/2}$.

A. Contractions

The contracted product of tensors is a generalization of the inner product [25]. For two tensors $\mathcal{A} \in \mathbb{R}^{I_1 \times \ldots \times I_D \times J_1 \times \ldots \times J_M}$ and $\mathcal{B} \in \mathbb{R}^{K_1 \times \ldots \times K_L \times J_1 \times \ldots \times J_M}$, their contractive product corresponding to contraction modes $D+1, \ldots, D+M$ and $L+1, \ldots, L+M$ of tensors $\mathcal{A}$ and $\mathcal{B}$, repectively, can be defined as follows [26]

$$\mathcal{C} = \langle \mathcal{A}, \mathcal{B} \rangle_{D+1,\ldots,D+M;L+1,\ldots,L+M} \qquad \text{(II.2)}$$

where

$$c_{i_1,\ldots,i_D,k_1,\ldots,k_L} = \sum_{1 \le j_k \le J_k} a_{i_1,\ldots,i_D,j_1,\ldots,j_M} b_{k_1,\ldots,k_L,j_1,\ldots,j_M}.$$

Obviously (II.2) defines a linear system of equations. Based on this definition, for oder-$2N$ tensor $\mathcal{A} \in \mathbb{R}^{I_1 \times \ldots \times I_N \times J_1 \times \ldots \times J_N}$ and order-N tensor $\mathcal{X} \in \mathbb{R}^{J_1 \times \ldots \times J_N}$, the contractive product

$$\mathcal{Y} = \langle \mathcal{A}, \mathcal{X} \rangle_{N+1:2N;1:N}, \qquad \text{(II.3)}$$

between contraction modes $N+1, \ldots, 2N$ and $1, \ldots, N$ of tensors $\mathcal{A}$ and $\mathcal{X}$, respectively, will be

$$y_{i_1,\ldots,i_N} = \sum_{\substack{1 \le j_k \le J_N \\ 1 \le k \le N}} a_{i_1,\ldots,i_N,j_1,\ldots,j_N} x_{j_1,\ldots,j_N}.$$

This contraction will be used in the following.

B. Matricization

A tensor can be *matricized* in many different ways. We use the approach used in [26], [27]. Let the set $\{1, \ldots, M\}$ of modes of order-M tensor $\mathcal{A}$ is partitioned into $\{r_1, \ldots, r_t\}$and $\{c_1, \ldots, c_l\}$ sets. The matricization $A^{(r_1,\ldots,r_t;c_1,\ldots,c_l)}$ of $\mathcal{A}$ has the following form [26]

$$A^{(r_1,\ldots,r_t;c_1,\ldots,c_l)}(i,j) = a_{i_1,\ldots,i_M},$$

where

$$\begin{aligned} j &= 1 + \sum_{k=1}^{t} (i_{r_k} - 1) J_k, \quad J_k = \prod_{k'=1}^{k-1} I_{r_{k'}}, \\ i &= 1 + \sum_{k=1}^{l} (i_{c_k} - 1) I_k, \quad I_k = \prod_{k'=1}^{k-1} I_{c_{k'}}. \end{aligned}$$

In special case, the matricization $A^{(n;1,\ldots,n-1,n+1,\ldots,M)}$ is named mode-n matricization and represented with $A^{(n)}$[26], [27]. It is abvious that in this matricization the element $a_{i_1 \cdots i_N}$ of $\mathcal{A}$ is mapped to the element (i_n, j) of the matrix $A^{(n)}$ where

$$j = 1 + \sum_{k=1,k\neq n}^{M} (i_k - 1) J_k, \quad J_k = \prod_{m=1,m\neq n}^{k-1} I_m. \qquad \text{(II.4)}$$

C. Higher order singular value decomposition

Higher order singular value decomposition (HOSVD) is one common extension of singular value decomposition to the tensors [24]. Using HOSVD, every order-M tensor $\mathcal{A} \in \mathbb{R}^{I_1 \times \cdots \times I_M}$ can be decomposed as

$$\mathcal{A} = \left(U^{(1)}, \cdots, U^{(M)}\right) \cdot \mathcal{S}, \qquad \text{(II.5)}$$

where orthogonal matrices $U^{(i)}$ are singular matrices of tensor $\mathcal{A}$. Here, $U^{(i)}$ is the left singular matrix of $A^{(i)}$. The core tensor $\mathcal{S}$ is a real tensor of the same dimensions as $\mathcal{A}$ and

$$\mathcal{S} = \left(U^{(1)\mathsf{T}}, \cdots, U^{(M)\mathsf{T}}\right) \cdot \mathcal{A}.$$

Although this core tensor is not diagonal as in the case of SVD of matrices, but satisfies the following conditions:

- Any two different slices along the same mode are orthogonal. This property of core tensor $\mathcal{S}$ is named as all orthogonality.
- The values $s_j^k = \|\mathcal{S}(:, \cdots, :, j, :, \cdots, :)\|$, where j is in the k^{th} mode of $\mathcal{S}$, are named mode-k singular values of $\mathcal{A}$. It can be shown that for every k

$$s_1^k \geq s_2^k \geq \cdots \geq s_n^k \geq 0, \quad k = 0, \cdots, M. \tag{II.6}$$

  are equal to the singular values of the matrix $A^{(k)}$. This means that the norms of the slices along every mode are ordered.

The ordering property (II.6) demonstrates that, in the same way as matrices, singular values measure the 'energy' of the tensor. So, it is easy to see that the energy of core tensor $\mathcal{S}$ focused on the elements of $\mathcal{S}$ with small indices, especially in $\mathcal{S}(1, 1, \cdots, 1)$. This property of HOSVD (similar to SVD) is very useful in the applications that encounter with denoising problem. So, if $U_{k_l}^{(l)}$ contains the first k_l columns of the l^{th} singular matrix and $\widetilde{\mathcal{S}} = \mathcal{S}(1 : k_1, \ldots, 1 : k_M)$, the following truncated HOSVD

$$\widetilde{\mathcal{A}} = \left(U_{k_1}^{(1)}, \cdots, U_{k_M}^{(M)}\right)_{1:M} \cdot \widetilde{\mathcal{S}},$$

is a rank-$(k_1, \cdots, k_{2M})$ approximation of $\mathcal{A}$. Although, this is not optimal rank-$(k_1, \ldots, k_M)$ approximation of A, but steel is a good approximation and we have

$$\|A - \widetilde{A}\|^2 \leq \sum_{i=1}^{M} \sum_{j=k_i+1}^{r_i} s_j^{(i)^2},$$

where r_i is the rank of $A^{(i)}$ [24].

D. Banded Toeplitz matrix

Toeplitz matrix is a specially structured matrix which the same elements appear in its diagonals. Matrix-vector multiplication for these matrices can be done in $O(n \log n)$. In this paper, we face with banded Toeplitz matrices as follows

$$T = \begin{pmatrix} t_0 & \cdots & t_{-m} & & 0 \\ \vdots & \ddots & & \ddots & \\ t_m & & & & t_{-m} \\ & \ddots & & \ddots & \\ 0 & & t_m & \cdots & t_0 \end{pmatrix} \in \mathbb{R}^{(2m+1)\times(2m+1)}, \tag{II.7}$$

and for simplicity we use the following notation $T = \mathtt{toepb}(t)$, where $t = [t_{-m}, \ldots, t_m]^\mathsf{T}$. Multiplieing the Toeplitz matrix T with the anti-identity matrix

$$J = \begin{pmatrix} 0 & & 1 \\ & \iddots & \\ 1 & & 0 \end{pmatrix}, \tag{II.8}$$

gives the following special Hankel matrix

$$TJ = \begin{pmatrix} 0 & & t_{-m} & & t_0 \\ & \iddots & & \iddots & \\ t_{-m} & & \iddots & & t_m \\ & \iddots & & \iddots & \\ t_0 & & t_m & & 0 \end{pmatrix}. \tag{II.9}$$

This relation can be generalized to multilevel block Toeplitz with Toeplitz blocks. For example, if A be a block Toeplitz matrix with Toeplitz blocks (BTTB), $A(J \otimes J)$ will be a Hankel matrix with Hankel blocks(BHHB). Also for Toeplitz matrix T its transpose will be

$$T^\mathsf{T} = JTJ. \tag{II.10}$$

These properties will be used in the folowing.

III. A TENSOR BASED PRECONDITIONER FOR IMAGE RESTORATION WITH ZERO BOUNDARIES

In this section, we use a tensor framework in the modeling of image restoration problem. We will show that this framework enables us to deal with two or three-dimensional images directly without folding them to the vectors and without dealing with complicated multilevel matrices. Also, based on the structure of the obtained tensor, for the first time, we introduce a new tensor-based preconditioner. We verify the performance of the proposed strategy and demonstrate that the complexity of computing and applying this new preconditioner is comparable with well-known matrix preconditioners.

If $\mathcal{X}, \mathcal{Y} \in \mathbb{R}^{n_1 \times \ldots \times n_N}$, denote the discrete N-dimensional true and blurred images, respectively, the discrete version of (I.1) becomes

$$y_{i_1,\ldots,i_N} = \sum_{-m_k^{(l)} \leq i_k - j_k \leq m_k^{(u)}} p_{i_1-j_1,\ldots,i_N-j_N} x_{j_1,\ldots,j_N}. \tag{III.1}$$

Here PSF array

$$\mathcal{P} = \left(p_{l_1,\ldots,l_n}\right) \in \mathbb{R}^{m_1 \times \ldots \times m_N} \qquad {\scriptstyle -m_k^{(l)} \leq l_k \leq m_k^{(u)} \atop 1 \leq k \leq N},$$

is nonzero part of the discrete version of PSF function $p(.)$ and $m_k = m_k^{(l)} + m_k^{(u)} + 1 \leq n_k$ denotes the length of PSF array in mode k. Also, $p_{0,\ldots,0}$, the weight of $x_{i_1,\ldots,i_N}$ in construction of $y_{i_1,\ldots,i_N}$, is called the center of the PSF array. In image restoration with zero boundaries the elements of $x_{j_1,\ldots,j_N}$, only for $1 \leq j_k \leq n_k$ could be nonzero. Therfore the image restoration model (III.1) with zero boundary conditions becomes as follows

$$y_{i_1,\ldots,i_N} = \sum_{\substack{-m_k^{(l)} \leq i_k - j_k \leq m_k^{(u)} \\ 1 \leq j_k \leq n_k}} p_{i_1-j_1,\ldots,i_N-j_N} x_{j_1,\ldots,j_N}.$$

It is easy to confirm that this equation can be reformulated as

$$y_{i_1,\ldots,i_N} = \sum_{1 \leq j_k \leq n_k} a_{i_1,\ldots,i_N,j_1,\ldots,j_N} x_{j_1,\ldots,j_N}, \tag{III.2}$$

where for every $1 \leq i_k, j_k \leq n_k$ and $1 \leq k \leq N$,

$$a_{i_1,\ldots,i_N,j_1,\ldots,j_N} = \begin{cases} p_{i_1-j_1,\ldots,i_N-j_N}, & -m_k^{(l)} \leq i_k - j_k \leq m_k^{(u)}; \\ 0, & \text{Otherwise.} \end{cases} \tag{III.3}$$

Now by definition of contraction product in (II.3), the image restoration model (III.2) could be represented as the following tensor equation

$$\mathcal{Y} = \langle \mathcal{A}, \mathcal{X} \rangle_{N+1:2N;1:N}\,, \tag{III.4}$$

where $\mathcal{A}$ is order-2N tensor with elements defined in (III.3). By the properties of tensor matricization if $\mathbf{y} = Y^{(1:N)}$ and $\mathbf{x} = X^{(1:N)}$, the tensor equation (III.4) can be reformulated as the following linear equation

$$\mathbf{y} = A\mathbf{x}.$$

Here, $A = A^{(1:N;N+1;2N)}$ has the multilevel banded Toeplitz structure [1]. Although these two models are equal, using tensor framework allows us to use new tools to deal with this problem. For example in the following, we use an approximation of the blurring tensor $\mathcal{A}$ to derive a new preconditioner, which can not be obtained with matrix framework. Since A is not guaranteed to be nonsingular, its least squares (LS) should be considered,

$$\min_{\mathbf{x}} \|A\mathbf{x} - \mathbf{y}\|.$$

Usually, iterative methods are used to solve this large structured and ill-posed linear equation. For this structured linear system, the matrix-vector multiplication can be done by FFT without a need to explicit form of the blurring matrix A. Unfortunately, despite these excellent properties, the convergence rate of iterative methods for image restoration is low and to speed up the convergence, preconditioning techniques should be used. Different kinds of preconditioning methods have been proposed for image restoration with zero boundaries in two and three dimensions. All of these preconditioners have been computed based on the structure of blurring matrix and try to approximate this blurring matrix in the subspace corresponding to signal space. In this section, we demonstrate that based on tensor modeling framework used in (III.4), one can obtain a novel preconditioner with a new viewpoint based on an approximation of the blurring tensor operator, which can not be achieved with the matrix modeling. Here, we show that truncated HOSVD of the structured tensor operator (III.3) can be used as a preconditioner. In the next section, we show that the truncated HOSVD of the blurring tensor in image restoration with zero boundary conditions can be calculated very fast and its computational cost is comparable with the other matrix preconditioners. Now consider the HOSVD of the blurring tensor $\mathcal{A}$ as follows

$$\mathcal{A} = \left(U^{(1)}, \ldots, U^{(2N)}\right)_{1:2N} \cdot \mathcal{S}.$$

This decomposition has the following intersecting properties that encourage us to use its truncated version as a regularized preconditioner.

- The first columns of singular matrices $U^{(i)}$ in every mode are smoother than the last ones. So, for an appropriate index k_i, $U_{k_i}^{(i)} = [\mathbf{u}_1^{(i)}, \ldots, \mathbf{u}_{k_i}^{(i)}] \in \mathbb{R}^{n_i \times k_i}$ which denotes the first k_i columns of $U^{(i)}$ has an important role in the reconstruction of the exact image. For example, consider 2D satellite image restoration test problem which is presented as the first test in the experimental section. Figure 1 shows the values $\mathbf{u}_1^{(1)} \in \mathbb{R}^{256}$ and $\mathbf{u}_{10}^{(1)} \in \mathbb{R}^{256}$ of the mode-1 singular matrix $U^{(1)} \in \mathbb{R}^{256\times256}$. It is clear that $u_1^{(1)}$ is more smoother than $u_{10}^{(1)}$.

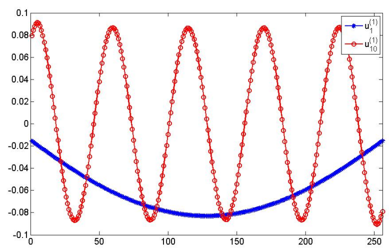

Fig. 1. The values of elements of vectors $\mathbf{u}_1^{(1)}$ and $\mathbf{u}_{10}^{(1)}$ for satellite test problem

- The most important parts of the core tensor $\mathcal{S}$ are located in the small indices. Also, these parts of the core tensor are corresponding to the smooth parts of the singular matrices. This means that if $\mathcal{S}_{\mathsf{k}} = \mathcal{S}(1:k_1, \ldots, 1:k_{2N})$ denotes the first part of the core tensor, for appropriate small indices k_i, $\|\mathcal{S}\|^2 - \|\mathcal{S}_{\mathsf{k}}\|^2$ will be small. Here, we use this notation $\mathsf{k} = (k_1, \ldots, k_{2N})$. For example Figure 2 shows the norm of $\mathcal{S}_{\mathsf{k}}$ when $k_i = j$ with different values of j for 2D satellite test problem. This behavior of core tensor $\mathcal{S}$ is the same as singular values of matrices for ill-posed problems. This means that for very small indices $\mathsf{k} = (k_1, \ldots, k_{2N})$, $\|\mathcal{S}\|^2 - \|\mathcal{S}_{\mathsf{k}}\|^2$ will be very small.

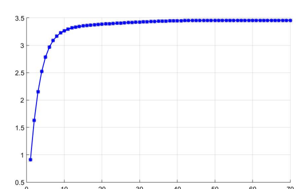

Fig. 2. The values of $\|\mathcal{S}_{\mathsf{k}}\|$ with $k_i = j, j = 1:70$ for satellite test problem

By these properties, the truncated HOSVD of the blurring operator $\mathcal{A}$ defined as

$$\mathcal{M} = \left(U_{k_1}^{(1)}, \ldots, U_{k_2}^{(2N)}\right)_{1:2N} \cdot \mathcal{S}_{\mathsf{k}} \tag{III.5}$$

is a good approximation of $\mathcal{A}$ corresponding to the smooth singular vectors of each mode and has regularization property. Also, for small values of k_i in k,

$$\|\mathcal{A} - \mathcal{M}\|^2 = \|\mathcal{S}\|^2 - \|\mathcal{S}_{\mathsf{k}}\|^2,$$

will be very small in ill-posed problems like image restoration problem. So this regularized approximation tensor $\mathcal{M}$ of the blurring tensor $\mathcal{A}$ can be used as a preconditioner. The matrix presentation of this preconditioner is $M = M^{(1:N;N+1:2N)}$, which explicitly becomes as follows:

$$M = U_{\mathsf{k}} S_{\mathsf{k}} V_{\mathsf{k}}^{\mathsf{T}}, \tag{III.6}$$

This article has been accepted for publication in a future issue of this journal, but has not been fully edited. Content may change prior to final publication. Citation information: DOI 10.1109/TIP.2017.2716840, IEEE Transactions on Image Processing

where

$$U_{\mathsf{k}} = \left(U^{(1)}_{k_1} \otimes \cdots \otimes U^{(N)}_{k_N}\right), V_{\mathsf{k}} = \left(U^{(N+1)}_{k_{N+1}} \otimes \cdots \otimes U^{(2N)}_{k_{2N}}\right),$$

and $S_{\mathsf{k}} = S^{(1:N;N+1:2N)}_{\mathsf{k}}$. Since this preconditioner is singular, so its pseudo-inverse $M^{\dagger}$ should be used in preconditioning process instead of M^{-1}, and so preconditioned LS restoration problem is

$$\min_{\mathbf{x}} \|M^{\dagger}A\mathbf{x} - M^{\dagger}\mathbf{y}\|.$$

Therefore at each step of a preconditioned iterative methods like Preconditioned CGLS (PCGLS), we should compute $\mathbf{q} = M^{\dagger}\mathbf{z}$ for some vectors z. This is equal to finding the solution with minimum length of the following least squares problem

$$\min_{z} \|M\mathbf{q} - \mathbf{z}\|.$$

Due to the orthogonality of U_{k} and V_{k}, the solution with minimum length of this least squares problem will be $\mathbf{q} = V_{\mathsf{k}}\overline{\mathbf{q}}$, where $\overline{q}$ is the solution of the following small least squares problem

$$\min_{\overline{\mathbf{q}} \in \mathbb{R}^{|\mathsf{k}|}} \|S_{\mathsf{k}}\overline{\mathbf{q}} - \overline{\mathbf{z}}\|, \quad \overline{\mathbf{z}} = U_{\mathsf{k}}^{\mathsf{T}}\mathbf{z} \in \mathbb{R}^{|\mathsf{k}|}, \quad |\mathsf{k}| = k_1k_2...k_N.$$

Since for ill-posed problems $|k|$ is very small in comparison with the dimension of A, i.e., $n = n_1...n_N$, the complexity of this LS problem is very small and negligible. Now, the important problem is the computational complexity of computing of this new tensor-based preconditioner, (i.e., truncated HOSVD of $\mathcal{A}$). In the following, we show that for image restoration with zero boundary conditions, this preconditioner can be constructed very fast. It should be mentioned that the other approximations of the blurring tensor that have regularization property may be used as a preconditioner.

A. Fast Truncated HOSVD Preconditioner

The main problem in using the HOSVD based preconditioners (III.6) or (III.5) is the complexity of computing the singular matrices U_{k_i} and core tensor $\mathcal{S}_{\mathsf{k}}$. Although the complexity of HOSVD of the blurring operator $\mathcal{A}$ is less than SVD of its corresponding matrix A, still it is very high for the preconditioning purpose. In this section, we show that for image restoration problem with zero boundary conditions this HOSVD based preconditioner could be found very fast. This is based on the existence of redundant and zero columns in matricization of the blurring operator in each mode. The following issues help us to compute the proposed preconditioner very fast:

- **Acceleration in computing singular matrices $U^{(i)}_{k_i}$:** For every i, the singular matrix $U^{(i)}$ of $\mathcal{A}$ is equal to the left singular matrix of the matricization $A^{(i)}$. In the following, we show that $A^{(i)}$ contains some zero and redundant columns that can be ignored in computing its left singular matrix. Here $A^{(i)}$ will be substituted with a smaller matrix $\overline{A}^{(i)}$ which causes a significant reduction in computational load of the singular matrices.
- **Relation between the singular matrices:** For an order-2N blurring operator $\mathcal{A}$, we show that $U^{(N+i)} = JU^{(i)}$. This relation means that only the first N singular matrices of $\mathcal{A}$ should be computed which causes a significant reduction in the elapsed time. Also we show that the singular values of $A^{(i)}$ and $A^{(N+i)}$ are equal.
- **Partially symmetric core tensor$\mathcal{S}$:** For elements of core tensor $\mathcal{S}$ we have $s_{i_1,\ldots,i_N,j_1,\ldots,j_N} = s_{j_1,\ldots,j_N,i_1,\ldots,i_N}$ which is a kind of partially symmetry property in tensors. So computing the elements $s_{i_1,\ldots,i_N,j_1,\ldots,j_N}$ with $i_l \leq j_l$ is enough.
- **Acceleration in computation of singular matrices by Lanczos bidiagonalization:** In computing the preconditioning matrix M, for ill-posed problems, only $k_l << n$ singular vectors of $U^{(i)}$ are needed. To speed up the construction process, one can use Lanczos Golub-Kahan bidiagonalization on $\overline{A}^{(i)}$ to approximate these singular vectors[28], [3].

The first three mentioned issues demonstrate that the complexity of computing the proposed preconditioner for the image restoration problem with zero boundary condition is less than the general case. Also, by the approach described in the last issue, this process even can be accelerated.

In the following, we prove the first three mentioned facts which will be summarized in lemma III.2. Then, the fourth issue, i.e., the acceleration based on Lanczos bidiagonalization will be described. The central part of computing HOSVD is the calculation of the singular matrices $U^{(i)}$. For every i, $U^{(i)}$ is the left singular matrix of $A^{(i)}$. Here, we show that for every i, $A^{(i)}$ contains some zero and redundant columns which helps us to derive a fast method for computing the singular matrices. Although in this paper, we consider 2D image restoration problem (N=2), it can be generalized to 3D image restoration problem (N=3). If we consider $A^{(1)}$, which is the matricization of $\mathcal{A}$ in mode-1, its columns will be

$$A^{(1)}(:, i_2 + (i_3 - 1)n_2 + (i_4 - 1)n_1n_2) = \mathcal{A}(:, i_2, i_3, i_4).$$

By this equation and definition of $\mathcal{A}$ in III.3, these columns are zero if $i_2 - i_4 \geq m_2^{(u)}$ or $i_2 - i_4 \leq -m_2^{(l)}$. Also, for every i_3, the columns of this matrix with similar $i_2 - i_4$ are equal. For every $1 \leq i_2, i_4 \leq n_2$, $i_2 - i_4$ could be one of the following numbers,

$$1 - n_2, \cdots, 0, \cdots, n_2 - 1.$$

which, their corresponding repetitions are

$$1, \cdots, n_2 - 1, n, n_2 - 1, \cdots, 1.$$

Since the columns of $\mathcal{A}(:, i_2, i_3, i_4)$ of $A^{(1)}$ can be nonzero only for $-m_2^{(l)} \leq i_2 - i_4 \leq m_2^{(u)}$, for every i_3, the distinct nonzero columns of $A^{(1)}$ are

$$\begin{aligned}\mathcal{A}(:, 1, i_3, m_2^{(l)} + 1), \cdots, \mathcal{A}(:, 1, i_3, 2), \mathcal{A}(:, 1, i_3, 1),\\ , \mathcal{A}(:, 2, i_3, 1), \cdots, \mathcal{A}(:, m_2^{(u)} + 1, i_3, 1),\end{aligned}$$

that their repetitions in $A^{(1)}$, are

$$n_2 - m_2^{(l)} + 1, \cdots, n_2 - 1, n_2, n_2 - 1, \cdots, n_2 - m_2^{(u)} + 1.$$

By moving i_3, from 1 to n_1, all distinct columns of $A^{(1)}$, can be presented as the following:

$$\begin{aligned}B_1 = [\mathcal{A}(:, 1, :, m_2^{(l)} + 1), \cdots, \mathcal{A}(:, 1, :, 2), \mathcal{A}(:, 1, :, 1),\\ , \mathcal{A}(:, 2, :, 1), \cdots, \mathcal{A}(:, m_2^{(u)} + 1, :, 1)].\end{aligned}$$

This article has been accepted for publication in a future issue of this journal, but has not been fully edited. Content may change prior to final publication. Citation information: DOI 10.1109/TIP.2017.2716840, IEEE Transactions on Image Processing

Also if

$$d_2 = \mathsf{diag}(\sqrt{n_2 - m_2^{(l)} + 1}, \cdots, \sqrt{n_2 - 1}, \sqrt{n_2}, \\ , \sqrt{n_2 - 1}, \cdots, \sqrt{n_2 - m_2^{(u)} + 1}),$$

and

$$D_1 = d_2 \otimes I, \tag{III.7}$$

the i^{th} diagonal element of D_1^2 denotes, the repetition of i^{th} column of B_1 in $A^{(1)}$. It's clear from definition of $\mathcal{A}$ in (III.3) that for every i, j, $\mathcal{A}(:, i, :, j)$ is a banded Toeplitz matrix as follows:

$$\mathcal{A}(:, i, :, j) = \mathsf{toepb}(P(:, i - j)).$$

Therefore B_1 becomes

$$B_1 = [\mathsf{toepb}(P(:, -m_2^{(l)})), \cdots, \mathsf{toepb}(P(:, m_2^{(u)}))]. \tag{III.8}$$

In the following lemma, we show that the singular values and left singular matrix of $A^{(1)} \in \mathbb{R}^{n_1 \times n_1 n_2^2}$ and the following smaller matrix

$$\overline{A}^{(1)} = B_1 D_1 \in R^{n_1 \times n_1 m_2}, \tag{III.9}$$

are equal. Here $n_1 m_2 << n_1 n_2^2$.

Lemma III.1. *Let $A = [a_1, \cdots, a_n]$ be a matrix with some redundant columns and $B = [a_{\sigma_1}, \cdots, a_{\sigma_k}]$ be a matrix constructed by nonzero columns of A without redundancy, where σ is a permutation on $\{1, \cdots, n\}$ and $k \le n$. If $D = diag(\sqrt{d_1}, \cdots, \sqrt{d_k})$, where d_k denotes the amount of repetitions of column a_{σ_k} on matrix A, we have*

$$AA^\mathsf{T} = BD^2B^\mathsf{T}$$

and, so the singular values and left singular vectors of A and BD are equal.

Proof. Without loss of generality, suppose that $\sigma_i = i$. Now

$$AA^\mathsf{T} = \sum_{i=1}^{n} a_i a_i^\mathsf{T}.$$

Since column a_i, repeated d_i times in matrix A, it can be written as

$$AA^T = \sum_{i=1}^{k} d_i a_i a_i^\mathsf{T} = BD^2B^\mathsf{T}.$$

This complete the proof. □

This fact used in [29] to remove redundant columns in the calculation of HOSVD of other structured tensors. So, by this lemma for computing the singular values and left singular vectors of $A^{(1)} \in \mathbb{R}^{n_1 \times n_1 n_2^2}$, one can use smaller matrix $\overline{A}^{(1)} \in \mathbb{R}^{n_1 \times n_1 m_2}$. If $A^{(2)}$ denotes the matricization of $\mathcal{A}$ in mode-2, By the same discussion as mode-1, one can prove that, the singular values and left singular vectors of matricization $A^{(2)}$ are equal to the singular values and singular vectors of

$$\overline{A}^{(2)} = B_2 D_2,$$

where

$$B_2 = [\mathsf{toepb}(P(-m_1^{(l)}, :)), \cdots, \mathsf{toepb}(P(m_1^{(u)}, :))], \tag{III.10}$$

denotes the distinct nonzero columns of $A^{(2)}$. Here i^{th} diagonal element of D_2^2 denotes the amount of repetition for the i^{th} diagonal of B_2 in the matrix $A^{(2)}$ and defined as follows:

$$D_2 = d_1 \otimes I, \tag{III.11}$$

where

$$d_1 = \mathsf{diag}(\sqrt{n_1 - m_1^{(l)} + 1}, \cdots, \sqrt{n_1 - 1}, \sqrt{n_1}, \\ , \sqrt{n_1 - 1}, \cdots, \sqrt{n_1 - m_1^{(u)} + 1}).$$

By continuing this process on modes 3 and 4, it can be shown that the singular values and left singular matrices of $A^{(3)}$ and $A^{(4)}$ are equal to those of

$$\overline{A}^{(3)} = B_3 D_1, \quad \overline{A}^{(4)} = B_4 D_2,$$

where

$$\begin{aligned} B_3 &= [\mathsf{toepb}(P(:, -m_2^{(l)}))^\mathsf{T}, \cdots, \mathsf{toepb}(P(:, m_2^{(u)}))^\mathsf{T}], \\ B_4 &= [\mathsf{toepb}(P(-m_1^{(l)}, :))^\mathsf{T}, \cdots, \mathsf{toepb}(P(m_1^{(u)}, :))^\mathsf{T}]. \end{aligned}$$

From property (II.10) of Toeplitz matrices, for every i, j we have

$$\begin{aligned} \mathsf{toepb}(P(:, i))^\mathsf{T} &= J\mathsf{toepb}(P(:, i))J \quad -m_2^{(l)} \le i \le m_2^{(u)}, \\ \mathsf{toepb}(P(j, :))^\mathsf{T} &= J\mathsf{toepb}(P(j, :))J \quad -m_1^{(l)} \le j \le m_1^{(u)}, \end{aligned}$$

which proves the following relations

$$B_3 = JB_1(I \otimes J), \quad B_4 = JB_2(I \otimes J).$$

Therefore

$$\begin{aligned} \overline{A}^{(3)} &= JB_1(I \otimes J)D_1, \\ \overline{A}^{(4)} &= JB_2(I \otimes J)D_2. \end{aligned}$$

For $i = 1, 2$ it is easy to see that $(I \otimes J)D_i = D_i(I \otimes J)$, which results the following relations:

$$\begin{aligned} \overline{A}^{(3)} &= J\overline{A}^{(1)}(I \otimes J), \\ \overline{A}^{(4)} &= J\overline{A}^{(2)}(I \otimes J). \end{aligned} \tag{III.12}$$

Since J and $(I \otimes J)$ are orthogonal and symmetric matrices, if $\overline{A}^{(1)} = U^{(1)}\Sigma^{(1)}V^{(1)\mathsf{T}}$ be the SVD of $\overline{A}^{(1)}$, from (III.12), the SVD of $\overline{A}^{(3)}$ becomes as follows

$$\overline{A}^{(3)} = JU^{(1)}\Sigma^{(1)}\overline{V}^{(1)\mathsf{T}}, \quad \overline{V}^{(1)} = (I \otimes J)V^{(1)}. \tag{III.13}$$

This shows that the sigular values of $\overline{A}^{(3)}$ and $\overline{A}^{(1)}$ are equal and the left singular matrix of $\overline{A}^{(3)}$ is the permutation of the left singular matrix of $\overline{A}^{(1)}$ by matrix J. The same relation between $\overline{A}^{(2)}$ and $\overline{A}^{(4)}$ can be obtained. Explicitly, if $N = 2$

$$U^{(i+N)} = JU^{(i)}, \quad \Sigma^{(i+N)} = \Sigma^{(i)}, \quad i = 1, 2. \tag{III.14}$$

By these relations and definition of $\mathcal{S}$ we have

$$\mathcal{S} = \left(U_1^\mathsf{T}, U_2^\mathsf{T}, U_1^\mathsf{T}J, U_2^\mathsf{T}J\right)_{1:4} \cdot \mathcal{A}. \tag{III.15}$$

Now, let $S = S^{(1:2;3:4)}$ be the marization of $\mathcal{S}$. Therefore from (III.15), we have

$$S = (U_1 \otimes U_2)^\mathsf{T}\widetilde{A}(U_1 \otimes U_2), \tag{III.16}$$

This article has been accepted for publication in a future issue of this journal, but has not been fully edited. Content may change prior to final publication. Citation information: DOI 10.1109/TIP.2017.2716840, IEEE Transactions on Image Processing

where $\widetilde{A} = A(J \otimes J)$. Since A is a BTTB matrix, from section II-D $\widetilde{A}$ becomes a BHHB matrix and so it is a symmetric matrix. It is obvious from (III.16) that S preserve this structure of $\widetilde{A}$ and becomes a symmetric matrix. By definition of tensor matricization, the elements of $S = S^{(1:2;3:4)}$ are

$$S(i_1 + (i_2 - 1)n_1, j_1 + (j_2 - 1)n_1) = s_{i_1,i_2,j_1,j_2}. \quad \text{(III.17)}$$

Since S is a symmetric matrix, we have

$$S(i_1+(i_2-1)n_1, j_1+(j_2-1)n_1) = S(j_1+(j_2-1)n_1, i_1+(i_2-1)n_1),$$

which from (III.17), gives

$$s_{i_1,i_2,j_1,j_2} = s_{j_1,j_2,i_1,i_2}. \quad \text{(III.18)}$$

This property of core tesnor $\mathcal{S}$ is a kind of partial symmetry in tensors. Therefore in computing the core tensor $\mathcal{S}$, the calculation of all elements is not necessary. These results can summarize in the following lemma

Lemma III.2. *Let $X, Y \in \mathbb{R}^{n_1 \times n_2}$ denote true and blurred images with PSF array $P \in \mathbb{R}^{m_1 \times m_2}$, then, the singular matrices $U^{(i)}, i = 1, \ldots, 4$ of HOSVD for the blurring tensor operator in* (III.2) *can be obtained as follows: $U^{(1)}$ and $U^{(2)}$ are the left singular matrices of the matrices $\overline{A}^{(i)} = B_i D_i$, where D_i and B_i for $i = 1, 2$ are defined in* (III.8), (III.10) , (III.7) *and* (III.11). *Also singular matrices $U^{(3)}$ and $U^{(4)}$ are*

$$U^{(3)} = JU^{(1)}, \quad U^{(4)} = JU^{(2)}.$$

Here matrix J is the anti-diagonal matrix defined in (II.8). *Also core tensor $\mathcal{S}$ is a partial symmetric tensor which satisfies in* (III.18).

In this lemma, it has been shown that the singular vectors in each mode of the blurring tensor can be obtained faster than general case. For special PSF arrays, this process even can be faster. For example, when PSF array is symmetric, the complexity of the proposed method could be reduced. PSF array $\mathcal{P} \in \mathbb{R}^{m_1 \times \ldots \times m_N}$ is symmetric if $m_i^{(l)} = m_i^{(u)} = \overline{m}_i$ and

$$p_{i_1,\ldots,i_N} = p_{i_1',\ldots,i_N'}, \quad \text{(III.19)}$$

if $i_k = \pm i_k'$ for $k = 1 \leq k \leq N$. Well-known PSF arrays, such as Gaussian PSF, satisfy this property. It is obvious from (III.19) that for symmetric PSF arrays, the number of distinct columns of matricizations of $\mathcal{A}$ in every mode will be reduced. For example, it is clear from (III.8) and (III.19) that for 2D case, all block matrices $\mathsf{toepb}(P(:, i))$ are symmetric and for $0 \leq i \leq \overline{m}_2$, we have

$$\mathsf{toepb}(P(:, i)) = \mathsf{toepb}(P(:, -i)),$$

which causes a reduction in the number of distinct columns of B_1. So,

$$\widetilde{B}_1 = [\mathsf{toepb}(P(:, -\overline{m}_2)), \ldots, \mathsf{toepb}(P(:, 0))]$$

denotes the distinct columns of $A^{(1)}$ for symmetric PSF array. Also, diagonal elements of $\widetilde{D}_1^2$ denote the amount of redundancy for the columns of $\widetilde{B}_1$ in $A^{(1)}$, where

$$\widetilde{D}_1 = I \otimes \widetilde{d}_2,$$

and $\widetilde{d}_2 = \sqrt{2}\mathsf{diag}(\sqrt{n_2 - m_2 + 1}, \ldots, \sqrt{n_2})$. Therefore, the left singular matrices of $A^{(1)} \in \mathbb{R}^{n_1 \times n_1 n_2^2}$ and $\widetilde{A}^{(1)} = \widetilde{B}_1 \widetilde{D}_1 \in \mathbb{R}^{n_1 \times (n_1(m_2+1)/2)}$ are equal. Moreover, since the block matrices $\mathsf{toepb}(P(:, i))$ in B_1, are symmetric, by definition of B_3, we have $B_3 = B_1$. This gives the following relation

$$U_1 = JU_1.$$

The same results can be obtained for mode-2 and mode-4.

Although these results proved for 2D image restoration problems, all of them can be generalized to 3D image restoration with zero boundary conditions.

Accelerating the calculation of the HOSVD based preconditioner by Lanczos bidiagonalization: Lemma III.2 demonstrated a significant reduction in the computational cost of construction the proposed preconditioner. For ill-posed problems, like image restoration, we need a very small number of the singular vectors in the proposed preconditioner. This construction process could be accelerated more using the approximation of singular matrices $u_{k_i}^{(i)}$ by applying Lanczos Golub-Kahan bidiagonalization on the matrix $\overline{A}^{(i)}$ [3]. It is well-known that by this bidiagonalization process, one can find an appropriate approximation of singular matrix $U_{k_i}^{(i)}$[3], [28]. Here, in the l^{th} step of Lanczos bidiagonalization on $\overline{A}^{(i)}$, we have

$$\overline{A}^{(i)} \overline{V}_l^{(i)} = \overline{U}_{l+1}^{(i)} B_l^{(i)} \quad \text{(III.20)}$$

where $\overline{U}_{l+1}^{(i)} \in \mathbb{R}^{n_i \times (l+1)}, \overline{V}_l^{(i)}$ are orthogonal matrices and $B_l^{(i)} \in \mathbb{R}^{(l+1) \times l}$ is a lower bidiagonal matrix. Let $B_l^{(i)} = N_l^{(i)} \begin{pmatrix} \overline{\Sigma}_l^{(i)} \\ 0 \end{pmatrix} Q_l^{(i)\mathsf{T}}$ be the SVD of small matrix $B_l^{(i)}$. By substituting this decomposition in (III.20) we have

$$\overline{A}^{(i)} \overline{V}_l^{(i)} Q_l^{(i)} = \overline{U}_{l+1}^{(i)} N_l^{(i)} \begin{pmatrix} \overline{\Sigma}_l^{(i)} \\ 0 \end{pmatrix},$$

Therefore, $Y_{l+1}^{(i)} = \overline{U}_{l+1}^{(i)} N_l^{(i)}$ is an approximation of the first left $l+1$ singular vectors of $\overline{A}^{(i)}$, i.e, $U_{l+1}^{(i)} = [u_1^{(i)}, \ldots, u_{l+1}^{(i)}]$. More details about this approximation could be found in [28], [3]. Approximation of the singular vectors by Lanczos Golub-Kahan process has been used to find a fast and high-quality preconditioner in [3], [14]. By using this approximation, the approximated orthogonal matrix $Y_{k_i}^{(i)} \approx U_{k_i}^{(i)}$ can be used in our proposed preconditioner. Also, ill-posedness of the image restoration problem and blurring operator $\mathcal{A}$ causes the rapid decay of the singular values of its matricizations $\overline{A}^{(i)}$ and so the elements of core tensor $\mathcal{S}$. Hence, usually, for every i, k_i can be considered very small and so $k_i \ll n_i$. Therefore, the cost of computing $Y_{k_1}^{(1)}$ of the structured matrix $\overline{A}^{(1)} \in \mathbb{R}^{n_1 \times n_1 m_2}$ is from order $m_2 n_1 \log n_1$. For the matrix $\overline{A}^{(2)} \in \mathbb{R}^{n_2 \times n_2 m_1}$, this will be $O(n_2 m_1 \log n_2)$. From the above discussions, we can conclude that by using the proposed method, one can compute the proposed preconditioner very fast.

Although we discussed zero boundary condition, by this approximation process, the use of HOSVD based preconditioning for other boundaries becomes reasonable. Here some iterations of Lanczos bidiagonalization can be applied on matrix $A^{(i)}$ to obtain the approximations of the first singular vectors.

IV. Experimental Results

In this section, to illustrate the effectiveness of our proposed preconditioner, some experiments on image restoration problems have been reported. In all experiments, 1% white noise added to the blurred images. Although the proposed preconditioner can adjust with all iterative methods, in this section, we use CGLS and its preconditioned version [8]. Here we don't use any regularization method and only use the semi-convergency property of iterative methods like CGLS. Due to this property, iterative methods converge to the exact solution in first steps, and then start to diverge after some iterations. So the number of iterations becomes the regularization parameter for iterative methods [7]. To verify the quality of the proposed HOSVD based preconditioner (Hos), we compare its results with well-known preconditioners, i.e., the Kronecker product approximation preconditioners (Kron) [1], [15] and the Lanczos-based preconditioner (Lanc) [3], [14].

As the first example, we consider the satellite test problem. The true image, PSF array, and noisy blurred image can be seen in the Figure 3. We solved this image restoration problem

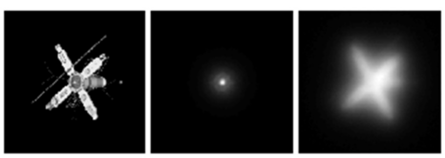

Fig. 3. Exact image, Gaussian blur and noisy blurred satellite test image from left to right, respectively

with CGLS and PCGLS with different preconditioners. Figure 4 shows the relative errors of restored images with these different methods in each iteration. It's clear from this figure

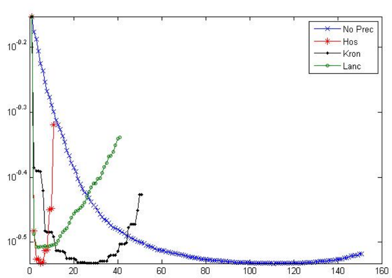

Fig. 4. The relative errors versus iterations for CGLS and PCGLS with Hos, Kron and Lanc preconditioners for satellite test problem.

that the proposed method can achieve better reconstruction in a small number of iterations. Also, the restored images in iteration 4 of all methods can be found in Figure 5. As the second test, we consider the satellite test problem with the PSF array presented in the Figure 6, [30]. We solved the restoration problem corresponding to this PSF array. The

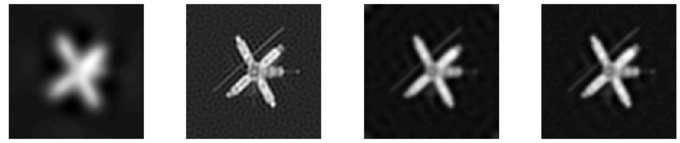

Fig. 5. Restored images at iteration 4 with No preconditioner, Hos, Kron and Lanc preconditioners, from left to right, respectively.

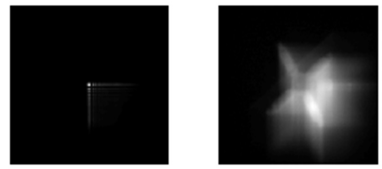

Fig. 6. The PSF array and noisy blurred satellite image in the second test, from left to right, respectively.

relative errors for different preconditioners are reported in the Figure 7. The minimum error of the Hos preconditioner

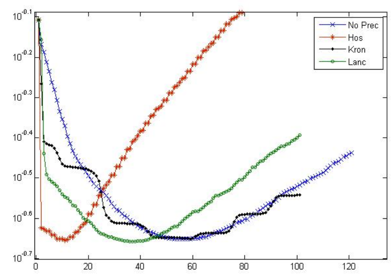

Fig. 7. The Relative errors versus iterations for CGLS and PCGLS with Hos, Kron and Lanc preconditioners for satellite image with the new PSF array in Figure 6

appears at iteration 10, which is less than the others. Figure 8 presents the restored images by these methods at iteration 10. For the third test problem, we consider the blurring of

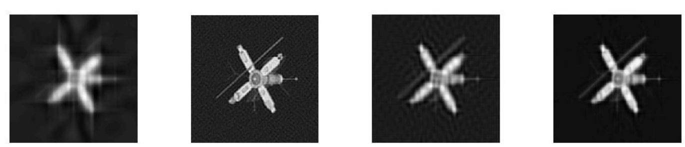

Fig. 8. Restored images at iteration 10 with No preconditioner, Hos, Kron and Lanc preconditioners, from left to right, respectively, for the second test problem.

the well-known cameraman test problem. The PSF array, exact and blurred images can be found in Figure 9. We solved this restoration problem using Kron, Lanc, and the proposed Hos preconditioners. Kron based preconditioner did not converge for this test problem and in the best case worked like No-preconditioner method. So, here we did not report its results. Figure 10 shows the obtained relative errors in different iterations. Also, figure 11 shows the restored images at iteration 8. Also, Table IV shows the elpased time of all

This article has been accepted for publication in a future issue of this journal, but has not been fully edited. Content may change prior to final publication. Citation information: DOI 10.1109/TIP.2017.2716840, IEEE Transactions on Image Processing

Fig. 9. The exact image, PSF array and blurred images for cameraman test image from left to right, respectively.

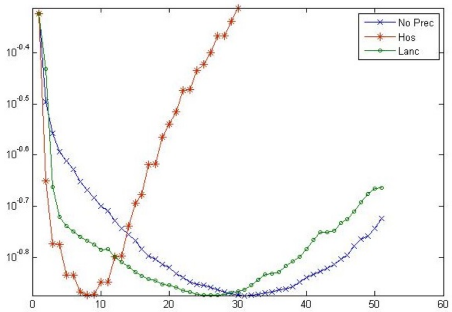

Fig. 10. The Relative errors versus iterations for CGLS and PCGLS with Lanc and Hos preconditioners for cameraman test problem

Fig. 11. The restored cameraman test problem at iterations 8 with CGLS and PCGLS with Hos and Lanc preconditioners, from left to right.

TABLE I
THE ITERATION AND TIME OF BEST RESTORATION OF ALL METHODS FOR 2D TEST PROBLEM

Method	Test1		Test2		Test3	
	iteration	time	iteration	time	iteration	time
No prec	118	5.125	60	3.20	31	1.69
Hos	4	0.425	10	1.01	8	0.81
Kron	27	1.51	59	2.32	-	-
Lanc	6	0.511	37	2.11	26	0.89

methods for all mentioned 2D test problems. As mentioned before, the proposed preconditioner can be used for 3D image restoration problem, too. Here we study the performance of the proposed preconditioner in the 3D case and verify the performance improvement in utilizing the proposed strategy. We use MRI test problem from MATLAB with different PSF arrays. In this test problem $\mathcal{X} \in \mathbb{R}^{64\times 64\times 20}$. First PSF array is considered as the mean of three Gaussian PSF with variances $1, 1.5$ and 2. Figure 12 shows the obtained relative errors with CGLS and PCGLS with Kron and the proposed Hos preconditioners. Also, we use another PSF array. Here the PSF array is considered as a uniform PSF array with radius 6. The obtained relative errors in different iteration with CGLS and PCGLS with 3D Kron and Hos preconditioners can be found in

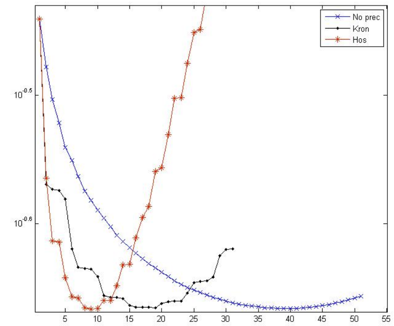

Fig. 12. The Relative errors versus iterations for CGLS and PCGLS with Hos and Kron preconditioners for MRI test with Gaussian like PSF array

Figure 13. It's clear from this figure that the Hos precondition

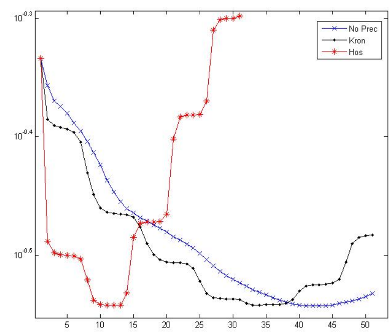

Fig. 13. The Relative errors versus iterations for CGLS and PCGLS with Hos and Kron preconditioners for MRI test with a uniform PSF array

can achieve its minimum error in iteration 11 which is less than the others. Some exact and blurred slices of MRI image and also restored images by different methods at iteration 11 could be found at figure 14. Also Table IV shows the elapsed time of all methods for MRI with Gussian (MRI(G)) and uniform (MRI(U)) tests.

TABLE II
THE ITERATION AND TIME OF BEST RESTORATION OF ALL METHODS FOR 3D PROBLEMS

Method	MRI(U)		MRI(G)	
	iteration	time	iteration	time
No prec	44	5.78	40	5.21
Hos	11	1.73	9	1.43
Kron	34	5.35	19	2.96

V. CONCLUSION

In this paper, we demonstrated that image restoration could be modeled with the tensor framework. Based on this context, we proposed a novel preconditioner based on using an approximation of the truncated HOSVD. We showed that due to the structure of the blurring tensor, this preconditioner could be constructed very fast. Also, experimental results confirm the

This article has been accepted for publication in a future issue of this journal, but has not been fully edited. Content may change prior to final publication. Citation information: DOI 10.1109/TIP.2017.2716840, IEEE Transactions on Image Processing

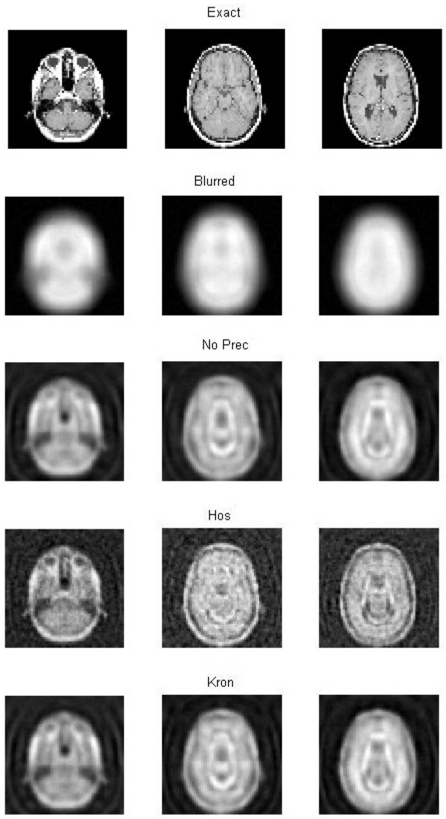

Fig. 14. Some slices of exact, blurred MRI image with uniform PSF array and restored slices with different methods at iteration 11

high quality of the proposed preconditioner in speeding up the convergence rate of iterative restoration methods and its outperformance compared with some state of the art preconditioners.

REFERENCES

[1] M. Rezghi, S. M. Hosseini, and L. Elden, “Best Kronecker product approximation of The blurring operator in three dimensional image restoration problems,“ *SIAM J. Matrix Anal. Appl.*, vol. 35, pp. 1086-1104, 2014.

[2] C. He, C. Hu, X. Li, and W. Zhang, “A parallel primal-doual splilitting method for image restoration“, *Information Science*, vol. 358, pp. 73-91, 2016.

[3] M. Rezghi, S. M. Hosseini, “Lanczos based preconditioner for discrete ill-posed problems,“*Computing*, vol. 88, pp. 79-96, 2010.

[4] P. C. Hansen, J. Nagy, and D. P. O’leary, Deblurring Images: Matrices, Spectra and Filtering, SIAM, Philadelphia, 2006.

[5] M. Hanke, J. Nagy, and R. Plemmons, “Preconditioned iterative regularization methods for ill-posed problems“, *in: Reichel L, Ruttan A, Varga RS (Eds.), Numerical Linear Algebra, 1993, de Gruyter, Berlin, Germany*, pp. 141-163.

[6] M. Hanke, Conjugate Gradient Type Methods for Ill-Posed Problems, Chapman and Hall/CRC, 1995.

[7] G. Landi, E. Loli Piccolomini, and I. Tomba, ”A stopping criterion for iterative regularization methods”, *Applied Numerical Mathematics*, vol. 106, pp. 53–68, 2016.

[8] A. Bjorck, Numerical Methods for Least Squares Problems, SIAM, 1996.

[9] Y. Saad, Iterative methods for sparse linear systems, SIAM, 2Ed, 2003.

[10] M. Rezghi, S. M. Hosseini, “An ILU preconditioner for nonsymmetric positive definite matrices by using the conjugate Gram-Schmidt process,“*Journal of Computational and Appled Mathematics*, vol. 188, pp. 150–164, 2006.

[11] P. Dell’Acqua, M. Donatelli, S. Serra-Capizzano, D. Sesana, and C. Tablino-Possio, “Optimal preconditioning for image deblurring with Anti-Reflective boundary conditions“, *Linear Algebra and its Applications*, vol.502, pp. 159–185, 2016.

[12] P. Dell’Acqua, M. Donatelli, and C. Estatico, “Preconditioners for image restoration by reblurring techniques“, *Journal of Computational and Applied Mathematics*, vol. 272, pp. 313–333, 2014.

[13] M. Hanke and J. Nagy , “Inverse Toeplitz preconditioners for ill-posed problems,“ *Linear Algebra and its Applications*, vol. 284, pp. 137–156, 1998.

[14] S. Erfani, A. Tavakoli, and D. K. Salkuyeh, “An efficient method to set up a Lanczos based preconditioner for discrete ill-posed problems“, *Applied Mathematical Modelling*, vol. 37, pp. 8742–8756, 2013.

[15] J. Kamm and J. G. Nagy, “Optimal kronecker product approximation of block Toeplitz matrices“, *SIAM J. Matrix Anal. Appl.*, vol. 22, pp. 155-172, 2000.

[16] J. G. Nagy, M. K. Ng, and L. Perrone, “Kronecker product approximations for image restoration with reflexive boundary conditions,“ *SIAM J. Matrix Anal. Appl.*, vol. 25, pp. 829- 841, 2003.

[17] L. Perrone, “Kronecker product approximations for image restoration with anti-reflective boundary conditions,“ *Numerical Linear Algebra with Applications*, vol. 13, pp. 1-22, 2005.

[18] X. L. Lv, T. Z. Huang, Z. B. Xu, and X. L. Zhao, “Kronecker product approximationes for image restoration with whole sample symmetric boundary conditiones“, *Information Science*, vol. 186, pp. 150-163,2012.

[19] J. G. Nagy and M. E. Kilmer, “Kronecker Product Approximation for Preconditioning in Three-Dimensional Image Applications“, *IEEE Transaction on Image Processing*, vol. 15, pp. 604-913, 2006.

[20] J. Liu, P. Musialski, P. Wonka, and J. Ye, “Tensor completion for estimating missing values in visual data“. *In ICCV, 2009,*pp. 2114–2121.

[21] Q. Xie, Q. Zhao, D. Meng, Z. Xu, S. Gu, W. Zuo, and L. Zhang, “Multispectral image denoising by intrinstic tensor sparsity regularization,“ *in CVPR, 2016*, pp. 1692–1700.

[22] D. Goldfarb, and Z. Qin, “Robust low-rank tensor recovery: models and algorithms,“ *SIAM J. Matrix Anal. Appl.,* vol. 35, pp. 225-253, 2014.

[23] V. De Silva and L. H. Lim, “Tensor rank and the ill-posedness of the best low-rank approximation problem“, *SIAM J. Matrix Anal. Appl.*, vol. 30, pp. 1084–1127, 2008.

[24] L. De Lathauwer, B. De Moor, and J. Vandewalle, “A multilinear singular value decomposition,“*SIAM J. Matrix Anal. Appl.*, vol. 21, pp.1253-1278, 2000.

[25] M. Rezghi and L. Elden, “Diagonalization of tensors with circulant structure,“ *Linear Algebra and Its Applications*, vol. 435, pp. 422–447, 2011.

[26] B. Bader and T. Kolda, “Algorithm 862: MATLAB tensor classes for fast algorithm prototyping,“*ACM Trans. Math. Softw.,* vol 32 , pp. 635–653, 2006.

[27] T. G. Kolda and B. W. Bader, “Tensor decompositions and applications“, *SIAM Review*, vol. 32, pp. 455–500, 2009.

[28] G. H. Golub and C. F. Van Loan, Matrix computation, The Johns Hopkins University Press, Baltimore,1996.

[29] R. Badeau and R. Boyer, “Fast multilinear singular value decomposition for structured tensors,“ *SIAM J. Matrix Anal. Appl.,* vol. 30, pp. 1008–1021, 2008.

[30] J. G. Nagy, K. Palmer, and L. Perrone, “Iterative methods for image Deblurring: A Matlab object-oriented approach,“ *Numerical Algorithms*, vol. 36 , pp. 73 – 93, 2004.

Mansoor Rezghi received B.Sc degree from Shahid Beheshti University in 2001, the M.Sc. degree and Ph.D. from Tarbiat Modares University, Tehran-Iran, in 2003 and 2008, respectively. Currently, he is an assistant professor of computer science at Trabiat Modares University since 2012. He is working on the matrix, Tensor and inverse problem techniques with applications in image processing and pattern recognition.